

## Lithium-iron micas from the Krušné hory Mountains (Erzgebirge): Twins, epitactic overgrowths and polytypes

By MILAN RIEDER\*

Department of Earth and Planetary Sciences, The Johns Hopkins University, Baltimore, Maryland

(Received March 11, 1970)

### Auszug

Röntgenaufnahmen an Glimmerzwillingen lassen die verschiedenen Orientierungen der Zwillingsindividuen erkennen, nicht deren Schichtfolgen. Dementsprechend werden Symbole für Glimmerzwillinge auf der Basis der möglichen Orientierungen vorgeschlagen. Dabei zeigt sich, daß die nicht häufigen Zwillinge nach  $[100]_{180^\circ}$  und  $[110]_{180^\circ}$  noch seltener sein mögen, als angenommen wird. Verzwilligung nach  $[100]_{180^\circ}$  infolge epitaktischer Verwachsung von FRANZINIS *A*- und *B*-Schichten wurde bei Lithium-Eisen-Glimmern nicht beobachtet. Es gibt Anzeichen dafür, daß Glimmer, die bei hoher Temperatur entstanden sind, vorzugsweise zur Verzwilligung neigen. Die Bedeutung der Wachstumsbedingungen für die Art der Stapelung wird durch die Epitaxie zwischen Zweiseicht- und *1M*-Strukturen und durch die Häufigkeit nach Zufall gestapelter Polytype in Glimmern solcher Vorkommen, die Bedingungen für regelloses Wachstum aufweisen, demonstriert.

Vier neue Polytype wurden identifiziert:  $5M [(222)2\bar{2}]$ ,  $14M [(222)_42\bar{2}]$ ,  $9Tc [(0)_72\bar{2}]$  und  $12M$ . Der Winkel  $\beta$  der *1M*-Untierzelle ändert sich systematisch: er ist am größten in *1M* und am kleinsten in  $2M_1$ . In allen anderen Polytypen liegt  $\beta$  zwischen diesen beiden Extremen; der Winkel kann aus der Stapelfolge eines Polytyps vorausgesagt werden. Das gilt für die Lithium-Eisen-Glimmer und zum Teil für Muskowit, nicht für Magnesium-Eisen-Glimmer.

Es werden Kriterien für den Nachweis der Zwillinge von *1M*, epitaktischen Verwachsungen zwischen *1M* und  $2M_1$ ,  $2M_2$ , sowie für die Unterscheidung zwischen Zwillingen, epitaktischen Verwachsungen und Polytypen angegeben.

### Abstract

When mica twins are identified from single-crystal x-ray photographs, numbers of participating individuals (= orientations), and not of their lamellae, are recognized. A system of mica-twin symbols is proposed on the basis of combinations of possible orientations. From this concept it follows that the infrequent twin elements  $[100]_{180^\circ}$  and  $[110]_{180^\circ}$  may be even less frequent than it had been thought. Twinning on  $[100]_{180^\circ}$  due to an epitactic coalescence of

\* Present address: Ústav geologických věd University Karlovy (Institute of Geological Sciences, Charles University), Albertov 6, Praha 2, Czechoslovakia.

FRANZINI's *A* and *B* layers was not found in lithium-iron micas. There are indications that twinning may be preferred by micas grown at high temperatures. The importance of growth conditions for the mode of stacking is indicated by the epitaxy between two-layer structures and  $1M$  and by the frequency of randomly stacked polytypes in micas from occurrences likely to produce conditions of chaotic growth.

Four new polytypes,  $5M[(222)2\bar{2}]$ ,  $14M[(222)_42\bar{2}]$ ,  $9Tc[(0)_72\bar{2}]$ , and  $12M$  were identified. The angle  $\beta$  of  $1M$  subcell varies systematically with polytypism: it is largest in  $1M$  and smallest in  $2M_1$ . In all other polytypes  $\beta$  lies between the two extremes and can be predicted if the stacking sequence of a polytype is known. This relation holds for lithium-iron micas and partly for muscovite; it does not hold for magnesium-iron micas.

Criteria for identification of twins of  $1M$ , epitactic overgrowths between  $1M$  and  $2M_1$ ,  $2M_2$ , as well as additional criteria for distinction between twins, epitactic overgrowths and polytypes are given.

## I. Introduction

The first part of the study of lithium-iron micas from the Krušné hory Mountains (Erzgebirge) dealt with chemical composition, cell parameters and optical properties<sup>1,2</sup>. In the course of that study, over one hundred crystals of lithium-iron micas were examined with a Buerger precession camera. This yielded new information on mica twins, epitactic overgrowths and polytypes, which is summarized in this paper.

## II. Twins

### 1. Review and discussion

Three twin laws have been known in the micas, on  $\langle 310 \rangle^3$ ,  $\langle 110 \rangle$  and  $\langle 100 \rangle$ , the last being identical with twinning on (001). It was argued<sup>4,5</sup> that these laws can be described equally well as rotations

<sup>1</sup> M. RIEDER, M. HUKA, D. KUČEROVÁ, L. MINAŘÍK, J. OBERMAJER and P. POVONDRA, Chemical composition and physical properties of lithium-iron micas from the Krušné hory Mts. (Erzgebirge) Part A: Chemical composition. *Contrib. Min. Petr.* **27** (1970) 131–158.

<sup>2</sup> M. RIEDER, A. PÍCHOVÁ, M. FASSOVÁ, E. FEDIUKOVÁ and P. ČERNÝ, Chemical composition and physical properties of lithium-iron micas from the Krušné hory Mts. (Erzgebirge) Part B: Cell parameters and optical data. *Mineral. Mag.* (in press).

<sup>3</sup> In discussion of twinning, symbols  $[hk0]$  and  $\langle hk0 \rangle$  represent  $[hk0]_{180^\circ}$  and  $\langle hk0 \rangle_{180^\circ}$ , respectively.

<sup>4</sup> R. SADANADA and Y. TAKÉUCHI, Polysynthetic twinning of micas. *Z. Kristallogr.* **116** (1961) 406–429.

<sup>5</sup> M. FRANZINI e L. SCHIAFFINO, Polimorfismo e leggi di geminazione delle biotiti. *Atti Soc. Toscana Sci. Nat. Pisa, Proc. Verbali Mem.* [A] **70** (1963) 60–98.

through multiples of  $60^\circ$  about the  $c^*$  axis. Although handy, this concept is inaccurate: Mica crystals are twinned rigorously on  $\langle hk0 \rangle$  axes, and the  $n \cdot 60^\circ$  ( $n \neq 3$ ) rotations about a perpendicular to (010) bring the individuals within a few minutes from their positions generated by twinning on  $\langle hk0 \rangle$ <sup>6</sup>.

Among mica twins, those on  $\langle 310 \rangle$  are most frequent. BELOV<sup>7</sup> predicted this on theoretical grounds: Twins on  $\langle 310 \rangle$  allow the whole twin to have a uniform packing of anions, which is close to cubic close packing<sup>8</sup>. The scarcity of the other two twin laws is due to a violation of anion packing on the interface of neighboring individuals, assumed by BELOV<sup>7</sup> to run through oxygen atoms sited at the apices of the (Si,Al)-O tetrahedra. SADANAGA and TAKÉUCHI<sup>4</sup> explained the infrequency of twins on  $\langle 110 \rangle$  and  $\langle 100 \rangle$  by a distortion of octahedral coordination polyhedra around interlayer cations. FRANZINI and SCHIAFFINO<sup>5</sup> considered such a distortion unlikely and argued that twins on  $\langle 110 \rangle$  and  $\langle 100 \rangle$  are possible only if built of two different mica layers, *A* and *B*. In such assemblages, octahedral coordination around interlayer cations is preserved, and the infrequency of such twins is then due to infrequency of *B* structures. One assemblage of *A* and *B* was reported by FRANZINI<sup>9</sup>.

According to any of the three concepts<sup>4,5,7</sup>, twins on  $\langle 110 \rangle$  and  $\langle 100 \rangle$  deserve more attention. It is desirable to recognize them with certainty. Besides, a set of criteria for identification of mica twins is needed to ascertain that twinning had been recognized prior to description of polytypes (discussed also in<sup>10</sup>). The two sets of identification criteria for twins of *1M* micas<sup>4,5</sup> permit an unequivocal identification of twins with two individuals (= orientations), but neither gives complete criteria for twins with more individuals.

<sup>6</sup> G. DONNAY, N. MORIMOTO, H. TAKEDA and J. D. H. DONNAY, Trioctahedral one-layer micas. I. Crystal structure of a synthetic iron mica. *Acta Crystallogr.* **17** (1964) 1369–1373.

<sup>7</sup> N. V. BELOV, On twin laws of micas and mica-like minerals. *Mineral. Sbornik L'vovsk. Geol. Obsheh.* **3** (1949) 29–40.

<sup>8</sup> From his concept of a quasi-cubic close anion packing, BELOV<sup>7</sup> predicted a sixfold coordination of interlayer cations and a ditrigonal arrangement of (Si,Al)-O tetrahedra. Expressions “anion” and “cation” are used for the sake of brevity; bonding in micas may not be purely ionic.

<sup>9</sup> M. FRANZINI, Nuovi dati sulla struttura delle miche triottaedriche. *Atti Soc. Toscana Sci. Nat. Pisa, Proc. Verbali Mem.* [A] **73** (1966) 620–631.

<sup>10</sup> J. V. SMITH and H. S. YODER, JR., Experimental and theoretical studies of the mica polymorphs. *Mineral. Mag.* **31** (1956) 209–235.

The point of confusion is that there are two stages in twin identification. Single-crystal x-ray photographs reveal orientations of individuals present in the assemblage; from orientations we interpret the twin law(s). Except in two-individual twins and a three-individual twin on  $\langle 310 \rangle$ , twin laws do not follow unequivocally from orientations detected. There is no self-apparent reason to expect lamellae of different individuals to alternate or group themselves in spirals as had been assumed<sup>4</sup>. An assemblage of crystals may involve several twin laws<sup>5</sup>, and we may fail to interpret them correctly. As an alternative to approaches in<sup>4,5</sup>, let us examine combinations of orientations and evaluate the corresponding presence criteria in terms of twin laws.

## 2. Twin symbols

Twin elements  $\langle 310 \rangle$ ,  $\langle 110 \rangle$  and  $\langle 100 \rangle$  applied on crystal orientation  $C$  (Fig. 1) produce five orientations,  $\bar{B}$ ,  $A$ ,  $\bar{C}$ ,  $B$ ,  $\bar{A}$ . Their labeling is analogous to that of single layers in polytypes<sup>11</sup>; to differentiate

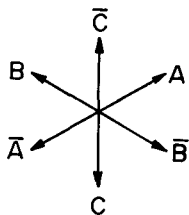


Fig. 1. Six possible orientations of the  $a$  vector of a  $1M$  mica unit cell projected along  $c^*$ . The labeling is analogous to that of  $ZVYAGIN$ <sup>11</sup>

crystals from single layers (marked by lower case letters in<sup>11</sup>), capital letters designate the former.

Unless the twin is cleaved and its portions x-rayed separately, single-crystal photographs do not permit the sequence of lamellae to be determined. So, the sequence of lamellae  $ABCBCBCB$  will read as  $ABC$ . Thus the presence criteria for twin identification by single-crystal photographs can be derived from combinations of  $R = 6$  orientations, taken  $r$  at a time

$$\binom{R}{r} = \frac{R!}{(R-r)!r!},$$

<sup>11</sup> B. B. ZVYAGIN, A theory of polymorphism of micas. *Kristallografiya* **6** (1961) 714–726; *Soviet Physics--Crystallography* **6** (1962) 571–580.

Table 1. Derivation of twins of 1M mica

$r$	$\begin{pmatrix} R \\ r \end{pmatrix}$ $R = 6$	Combinations of orientations	Twin symbol (vectors in Fig. 2)	Twin element(s) <sup>3</sup> or the minimum number of [100] and/or [110] operations (the rest may be [310], [100] or [110])	Presence criteria in Fig. 3
1	6	$C, \bar{B}, A, \bar{C}, B, \bar{A}$	$C$	none	$a$
2	15	$C\bar{B}, \bar{B}A, A\bar{C}, \bar{C}B, BA, AC, CA, \bar{B}\bar{C}, AB, CA, BC, AB, CC, B\bar{B}, AA$	$C\bar{B}$ $CA$ $C\bar{C}$	[110] [310] [100]	$b$ $c$ $d$
3	20	$C\bar{B}A, \bar{B}A\bar{C}, A\bar{C}B, \bar{C}B\bar{A}, B\bar{A}C, A\bar{C}\bar{B}, C\bar{B}C, BAB, ACA, \bar{C}B\bar{C}, B\bar{A}B, \bar{A}CA, \left. \begin{matrix} C\bar{B}\bar{B}, \bar{B}A\bar{A}, A\bar{C}\bar{C}, \bar{C}B\bar{B}, B\bar{A}\bar{A}, A\bar{C}\bar{C}, \\ CAB, \bar{B}CA \end{matrix} \right\}$	$C\bar{B}A$ $C\bar{B}\bar{C}$ $CAB$	at least one [110] one [110] and/or one [100] [310]	$e$ $f$ $g$
4	15	$C\bar{B}A\bar{C}, \bar{B}A\bar{C}B, A\bar{C}B\bar{A}, \bar{C}B\bar{A}C, B\bar{A}C\bar{B}, \bar{A}C\bar{B}A, C\bar{B}A\bar{B}, \bar{B}A\bar{C}A, A\bar{C}B\bar{C}, \bar{C}B\bar{A}B, B\bar{A}CA, \bar{A}C\bar{B}\bar{C}, C\bar{B}\bar{C}B, \bar{B}A\bar{B}A, A\bar{C}A\bar{C}$	$C\bar{B}A\bar{C}$ $C\bar{B}A\bar{B}$ $C\bar{B}\bar{C}B$	one [100] and/or at least one [110] one [100] and/or at least one [110] at least one [110] or [100]	$h$ $i$ $j$
5	6	$C\bar{B}A\bar{C}B, \bar{B}A\bar{C}B\bar{A}, A\bar{C}B\bar{A}C, \bar{C}B\bar{A}C\bar{B}, B\bar{A}C\bar{B}A, \bar{A}C\bar{B}A\bar{C}$	$C\bar{B}A\bar{C}B$	at least one [110] or [100]	$k$
6	1	$C\bar{B}A\bar{C}B\bar{A}$	$C\bar{B}A\bar{C}B\bar{A}$	at least one [110] or [100]	$l$

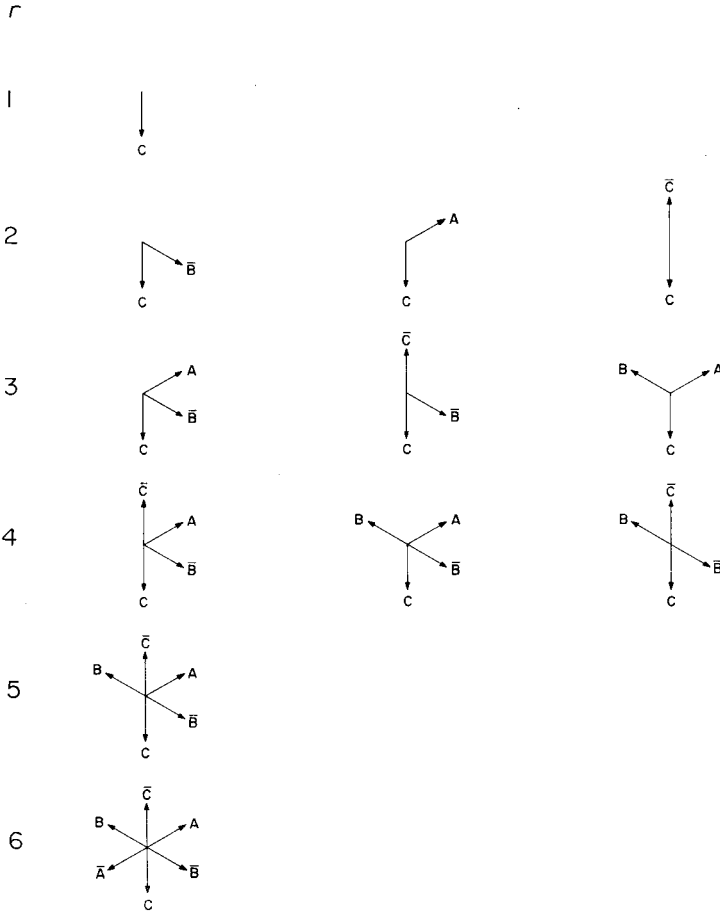
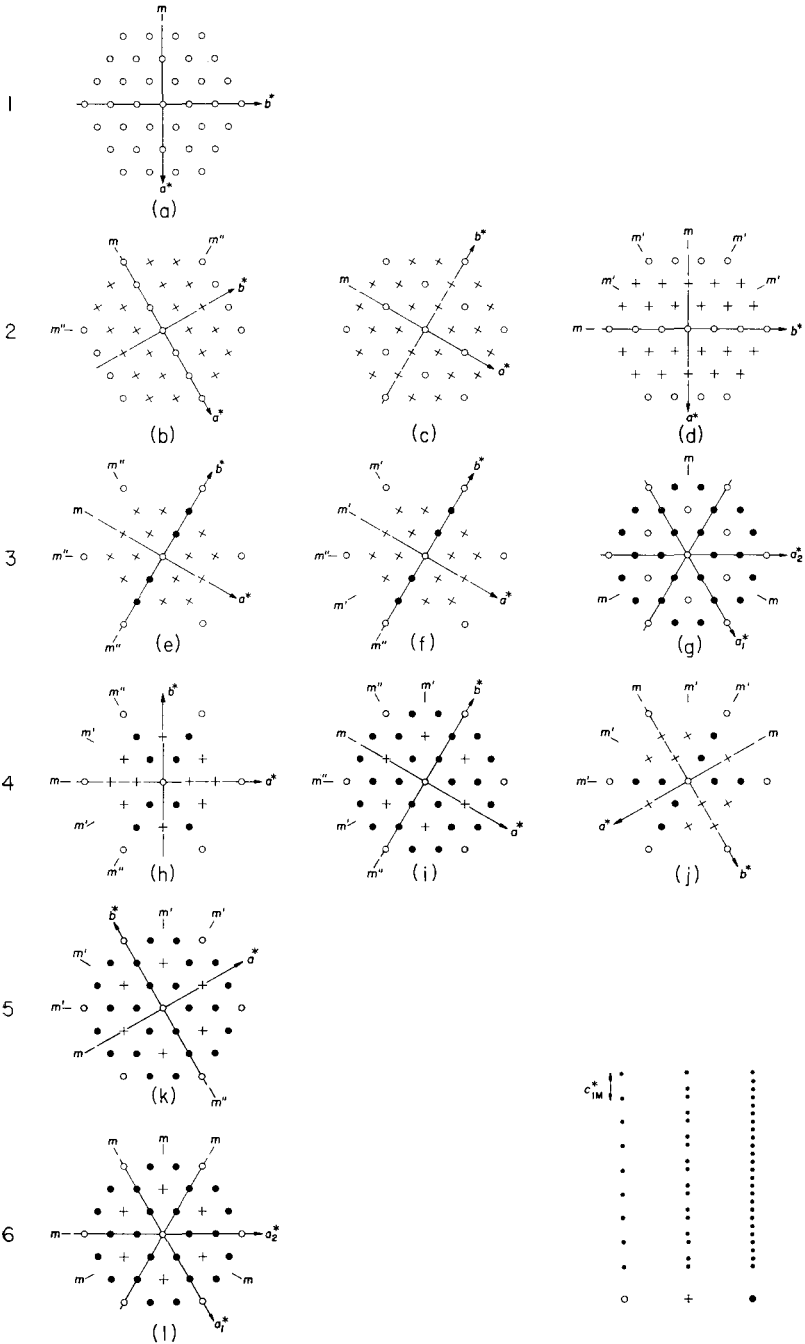


Fig. 2. Twelve combinations of orientations of 1M mica represented by vectors of Fig. 1;  $r$  stands for the number of orientations present

Fig. 3. Presence criteria corresponding to combinations of orientations of 1M mica given in Fig. 2. The criteria are shown as a projection of reciprocal lattices of participating individuals along  $c^*$ . Spacings in rows parallel  $c^*$  are shown in lower right-hand corner (not to scale with the rest of the figure). Being projected along  $c^*$ ,  $a^*_{1M}$  appears as  $1/a$  in length. Cases  $a, b, c, d, g$  and  $l$  are after SADANAGA and TAKÉUCHI<sup>4</sup>. Symbols:  $m$ —symmetry plane of the assemblage;  $m'$ —a geometrically rigorous symmetry plane that can be photographed only in a zero-level net perpendicular to the direction indicated;  $m''$ —a pseudo-symmetry plane that can be photographed only in a zero-level net perpendicular to the direction indicated; if  $\beta_{1M} = \delta$ ,  $m''$  cannot be distinguished from  $m'$

r



where  $1 \leq r \leq 6$ . These combinations include cases like  $C\bar{B}$ ,  $\bar{B}A$ ,  $A\bar{C}$ ,  $\bar{C}B$ ,  $B\bar{A}$ ,  $\bar{A}C$  (Table 1), all of which are twins on  $[\bar{1}10]$  of the first individual in each pair. Being twinned on one element, all might be represented by one symbol consisting of  $C$  followed by other orientations listed counterclockwise. The enantiomorphous  $C\bar{B}C$  and  $C\bar{B}B$  are a product of the same twin laws; it is sufficient to give the criteria for  $C\bar{B}C$  and to realize that their mirror image may exist. The vectors representing twin symbols of Table 1 are shown in Fig. 2, the corresponding presence criteria, in Fig. 3.

Presence criteria of Fig. 3 can distinguish all twelve cases if the angles in  $h0l_{1M}$  and  $h3hl_{1M}$  nets are not identical<sup>12</sup>. If these angles are identical or close to each other, criteria for cases  $i, k, l$  become identical and so do criteria for  $e$  and  $f$ . Thus in some cases we may fail to determine orientations involved in the assemblage.

Even if the orientations are known, the twin law follows in four cases only. In others, only twin operations necessarily present can be deduced. An examination of Table 1 and Fig. 2 reveals that in such cases twinning on  $\langle 110 \rangle$  and  $\langle 100 \rangle$  may not be as frequent as had been thought.

If more twin laws formed the assemblage (certainly the case in  $f, i, j$  of Fig. 3), we do not deal with a twin defined as<sup>13</sup> "... an assemblage of two or more crystals, symmetrical of one another with respect to a twin element". The name "complex twin" proposed in<sup>4</sup> is more appropriate. Another refinement of nomenclature should apply to assemblages containing  $A$  and  $B$  layers like the one reported by FRANZINI<sup>9</sup>. If unit cells of both structures are geometrically identical, the "twin" element brings to coincidence merely the lattices, not structures. As a consequence, such a case is not twinning, but epitaxy.

### 3. Twins observed in lithium-iron micas

Twins  $C\bar{B}$ ,  $CA$ ,  $C\bar{C}$ ,  $CAB$  and  $C\bar{B}A\bar{C}B\bar{A}$  or  $C\bar{B}A\bar{C}B$  or  $C\bar{B}AB$  were detected among the specimens studied (Table 2). The numbers of twins are low and prevent speculations about frequency of individual types. It should be mentioned that twin  $C\bar{B}AB$  has been reported<sup>14</sup> in a synthetic fluoro-polythionite.

<sup>12</sup> More discussion follows in IV.3 and V.

<sup>13</sup> J. D. H. DONNAY, *Crystallography*. The Encyclopedia Americana, Vol. VIII (1963) 277d.

<sup>14</sup> H. TAKEDA and J. D. H. DONNAY, Twinning and polytypism in lithium micas. Abstracts, Amer. Crystallogr. Assoc., February Meeting (1965) 23-24.

Table 2. *Twins found in lithium-iron micas*

Twin	Number of twins	Specimen
$\overline{CBACB\bar{A}}$ or $\overline{CB\bar{A}C\bar{O}B}$ or $\overline{CBAB}$	2	zinnwaldite, Krásno near Slavkov, Czechoslovakia (No. 38 in 1,2) (K, Rb, Cs) <sub>1.87</sub> Na <sub>0.09</sub> Ca <sub>0.04</sub> [Li <sub>1.01</sub> Fe <sub>1.30</sub> Mg <sub>0.04</sub> Mn <sub>1.07</sub> Al <sub>2.31</sub> Fe <sub>1.31</sub> <sup>+3</sup> ] Al <sub>1.71</sub> Si <sub>6.28</sub> Ti <sub>0.01</sub> O <sub>20.00</sub> [F <sub>1.81</sub> (OH) <sub>2.19</sub> ]
$\overline{CAB}$	1	} synthetic zinnwaldite, $\sim K_2Fe_2Li_2Al_2Si_6O_{20}F_4$ ; } grown from glass at 682½—685 °C and 2000 bars for 163 hours
$\overline{C\bar{B}}$	1	
$\overline{CA}$	2	zinnwaldite, Ehrenfriedersdorf, Germany (No. 30 in 1,2) (K, Rb, Cs) <sub>1.50</sub> Na <sub>0.14</sub> Ca <sub>0.05</sub> (H <sub>3</sub> O) <sub>.31</sub> [Li <sub>1.47</sub> Fe <sub>1.20</sub> Mg <sub>0.01</sub> Mn <sub>0.02</sub> Al <sub>2.17</sub> Fe <sub>1.71</sub> <sup>+3</sup> ] Al <sub>1.63</sub> Si <sub>6.36</sub> Ti <sub>0.03</sub> O <sub>20.00</sub> [F <sub>1.30</sub> (OH) <sub>2.70</sub> ]
	1	zinnwaldite, Cínovec, Czechoslovakia (No. 16 in 1,2) K <sub>1.08</sub> Rb <sub>0.11</sub> Na <sub>0.09</sub> Ca <sub>0.08</sub> (H <sub>3</sub> O) <sub>.64</sub> [Li <sub>1.83</sub> Fe <sub>1.37</sub> Mg <sub>0.03</sub> Mn <sub>0.07</sub> Al <sub>2.04</sub> Fe <sub>1.33</sub> <sup>+3</sup> ] Al <sub>1.69</sub> Si <sub>6.29</sub> Ti <sub>0.02</sub> O <sub>20.00</sub> [F <sub>2.75</sub> (OH) <sub>1.25</sub> ]
$\overline{C\bar{C}}$	2	zinnwaldite, Vysoký Kámen near Slavkov, Czechoslovakia (No. 37 in 1,2) (K, Rb, Cs) <sub>1.66</sub> Na <sub>0.06</sub> Ca <sub>0.10</sub> (H <sub>3</sub> O) <sub>.18</sub> [Li <sub>1.42</sub> Fe <sub>1.43</sub> Mn <sub>0.06</sub> Al <sub>2.12</sub> Fe <sub>1.33</sub> <sup>+3</sup> ] Al <sub>1.84</sub> Si <sub>6.15</sub> Ti <sub>0.01</sub> O <sub>20.00</sub> [F <sub>1.81</sub> (OH) <sub>2.19</sub> ]

Following FRANZINI<sup>9</sup>, intensities of eight  $h0l$  diffractions were measured for individuals in a  $C\bar{C}$  twin of a mica from Vysoký Kámen near Slavkov, Czechoslovakia. Its atomic coordinates were estimated from chemical composition and cell data according to the method of DONNAY *et al.*<sup>15</sup>. Structure factors were calculated for models *A* and *B*; those of *A* compare fairly well to the measured values for both individuals in the twin, those of *B* differ. The significance of this result, however, should not be overestimated; if the structure of zinnwaldite is octahedrally ordered<sup>16</sup>, its replacement by the model of <sup>15</sup> may be a serious oversimplification.

There are indications that mica twinning may be associated with a high-temperature origin. None of the crystals of synthetic fluoro-zinnwaldite that were grown at  $\sim 685^\circ\text{C}$  and 2 kbar was free from twins. No twins were found in a natural zinnwaldite from Cínovec (No. 22 in <sup>1,2</sup>) and in its crystals heated at low temperatures of for short periods of time. Twins were found, however, in a flake from this sample that was subjected to temperature  $\sim 705^\circ\text{C}$  and 2 kbar pressure for  $604\frac{1}{2}$  hours (not examined for twinning prior to treatment). The possible relation between twinning and high temperature is not opposed by chemical compositions of zinnwaldite twins listed in Table 2: The range of their  $\text{Li}/(\text{Li} + \text{Fe}^{+2})$  ratio is similar to that of synthetic lithium-iron micas found experimentally to have the highest temperature stability at 2 kbar<sup>17</sup>.

### III. Epitactic overgrowths

Precession photographs of several mica flakes could not be interpreted as those of twins of  $1M$ ,  $2M_1$  or as those of any of the known polytypes. Examination of many photographs and of the relative intensities of diffractions permitted to conclude that the photographs are those of oriented overgrowths including  $1M$ ,  $2M_1$ ,  $2M_2$ , and perhaps also  $3T$ .

Different polytypes or polymorphs coalescing in the edifice are not symmetry-related and the edifices cannot be called twins. They

---

<sup>15</sup> G. DONNAY, J. D. H. DONNAY and H. TAKEDA, Trioctahedral one-layer micas. II. Prediction of the structure from composition and cell dimensions. *Acta Crystallogr.* **17** (1964) 1374–1381.

<sup>16</sup> M. RIEDER, Zinnwaldite: Octahedral ordering in lithium-iron micas. *Science* **160** (1968) 1338–1340.

<sup>17</sup> M. RIEDER, A study of natural and synthetic lithium-iron micas. Ph. D. Thesis, Johns Hopkins University, Baltimore (1968).

are epitactic overgrowths as defined by RAMDOHR and STRUNZ<sup>18,19</sup> and join the overgrowths of mica and rutile, mica and chlorite<sup>20</sup>, and of the *A* and *B* mica layers<sup>5,9</sup>. The point at which the change of stacking takes place constitutes a fault in the sense of SMITH and YODER<sup>10</sup>.

Epitactic overgrowths  $1M$  and  $2M_1$ , and  $1M$  and  $2M_2$ , which were observed in micas from Cínovec and Radkovice (Czechoslovakia), respectively, produce characteristic rows parallel to  $c^*$  (Fig. 4) in most

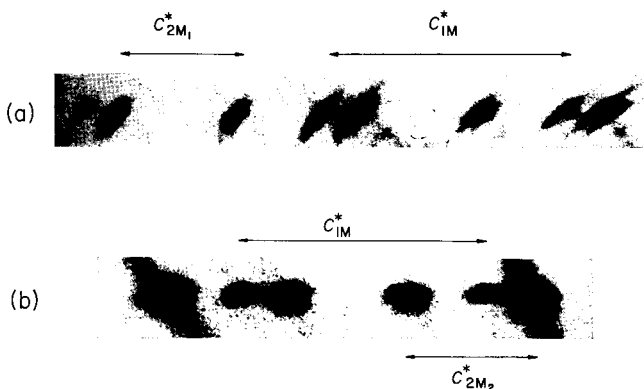


Fig. 4. Characteristic spacings in rows parallel to  $c^*$  of individuals in epitactic overgrowths of  $1M$  and two-layer structures. (a)  $02l_{2M_1}$  and  $11l_{1M}$  rows; zinnwaldite from Cínovec, Czechoslovakia; unfiltered copper  $K$  radiation. (b)  $02l_{2M_1}$  and  $13l_{1M}$  rows; trillithionite from Radkovice, Czechoslovakia; unfiltered molybdenum  $K$  radiation

$0kl_{2M}$ ,  $hhl_{2M}$  and  $h3hl_{2M}$ <sup>21</sup> reciprocal nets. Presence criteria for all possible mutual orientations of  $1M$  and  $2M$ <sup>21</sup> were derived by overlapping the respective nets; vectors and the corresponding presence criteria are summarized in Figs. 5–8. A case that might be an oriented overgrowth of  $3T$  and  $1M$  was also observed. As the  $c^*$  of both individuals

<sup>18</sup> P. RAMDOHR und H. STRUNZ, KLOCKMANN'S *Lehrbuch der Mineralogie*. Ferdinand Enke Verlag, Stuttgart (1967), p. 189.

<sup>19</sup> "Die orientierte Aufwachsung ist . . . als orientierte zweidimensionale Keimbildung auf dem Wirtkristall zu verstehen, wobei Wirt und Gast in der Verwachsungsebene einfache zweidimensionale (oder auch nur eindimensionale) Maschenanalogien aufweisen müssen"<sup>18</sup>.

<sup>20</sup> M. FRANZINI, R. MAZZUOLI e L. SCHIAFFINO, Flogopite e pennina in associazione parallela polisintetica (miniera del Ginevra, Isola d'Elba). *Atti Soc. Toscana Sci. Nat. Pisa, Proc. Verbali Mem. [A]* **73** (1966) 531–552.

<sup>21</sup> Symbol  $2M$  covers both  $2M_1$  and  $2M_2$ .

is not parallel, the case remains unsolved. A complex overgrowth built of five individuals was found in a lepidolite from Radkovice.

It is interesting to note that the "fault" angle in the two  $1M$  and  $2M$  overgrowths observed is identical with the stacking angle operating in one of the polytypes or polymorphs involved. An interpretation of the five-individual overgrowth from Radkovice was attempted assuming that the "fault" angle be either  $\sim 60^\circ$  or  $0^\circ$  (Fig. 9b); such an

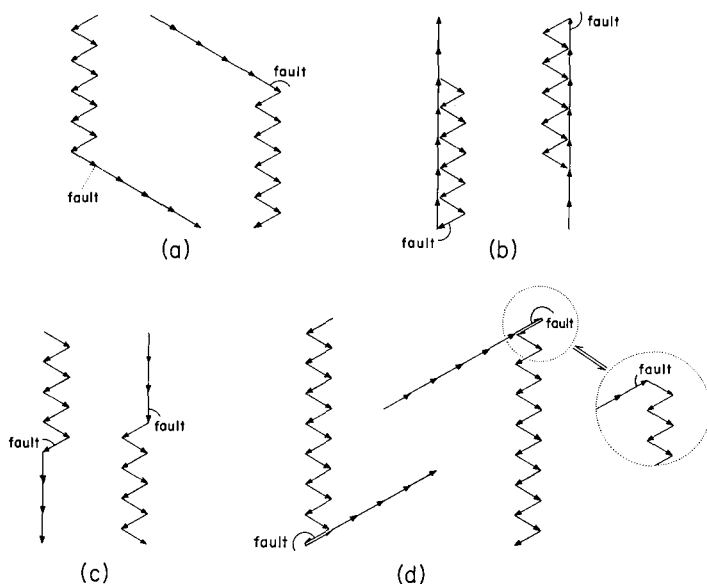


Fig. 5. Four possible epitaxial overgrowths of  $2M_1$  and  $1M$  shown by SMITH and YODER's<sup>10</sup> stacking vectors. An alternate interpretation of the stacking fault in case (d) is shown in a circle. Note that one  $3T$  repeat is completed on contact of  $2M_1$  and  $1M$  in (b)

interpretation is consistent with spiral growth. However, the only rigorous way of expressing the orientations of individuals in such assemblages is to use vectors (Fig. 9a).

The fact that a total of nine twins and five epitaxial overgrowths was found among one hundred crystals indicates that such overgrowths may be common. In fact, a photograph of a  $2M_1$  lepidolite from Nagatari, Japan, which was interpreted<sup>4</sup> as that of a twin of  $2M_1$ , resembles Fig. 4 rather than the theoretical  $2M_1$ -twin row or rows photographed by FRANZINI and SCHIAFFINO<sup>5</sup>.

## IV. Polytypes

## 1. Polytypes and polymorphs

Multiple stacking of mica layers has been referred to as polymorphism<sup>5,10,11,22-25</sup> and polytypism<sup>14,26,27</sup>.

The nomenclature is clear in dioctahedral micas such as muscovite:  $2M_1$  is by far the most frequent structure; very few structures are known, all with small repeats; transformation of  $1Md$ ,  $1M$ ,  $3T$  into

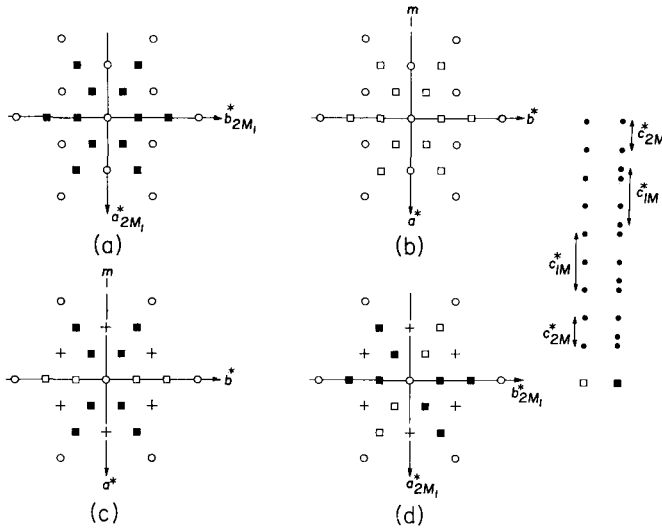


Fig. 6. Reciprocal lattices of  $2M_1$  and  $1M$  in epitactic overgrowths of Fig. 5 projected along  $c^*$ . Symbols as in Fig. 3, two additional symbols are explained on the right (not to scale with the rest of the figure). Note that single spacings (open circles) are single only in absence of “dioctahedral reflections” (see IV. 2, V)

<sup>22</sup> S. B. HENDRICKS and M. E. JEFFERSON, Polymorphism of the micas with optical measurements. *Amer. Mineralogist* **24** (1939) 729–771.

<sup>23</sup> A. A. LEVINSON, Studies in the mica group; relationship between polymorphism and composition in the muscovite-lepidolite series. *Amer. Mineralogist* **38** (1953) 88–107.

<sup>24</sup> N. GÜVEN and C. W. BURNHAM, The crystal structure of  $3T$  muscovite. *Carnegie Inst. Wash. Year Book* **65** (1967) 290–293.

<sup>25</sup> N. GÜVEN, The crystal structures of  $2M_1$  phengite and  $2M_1$  muscovite. *Carnegie Inst. Wash. Year Book* **66** (1968) 487–492.

<sup>26</sup> M. ROSS, H. TAKEDA and D. R. WONES, Mica polytypes: Systematic description and identification. *Science* **151** (1966) 191–193.

<sup>27</sup> H. TAKEDA, Determination of the layer stacking sequence of a new complex mica polytype: A 4-layer lithium fluorophlogopite. *Acta Crystallogr.* **22** (1967) 845–853.

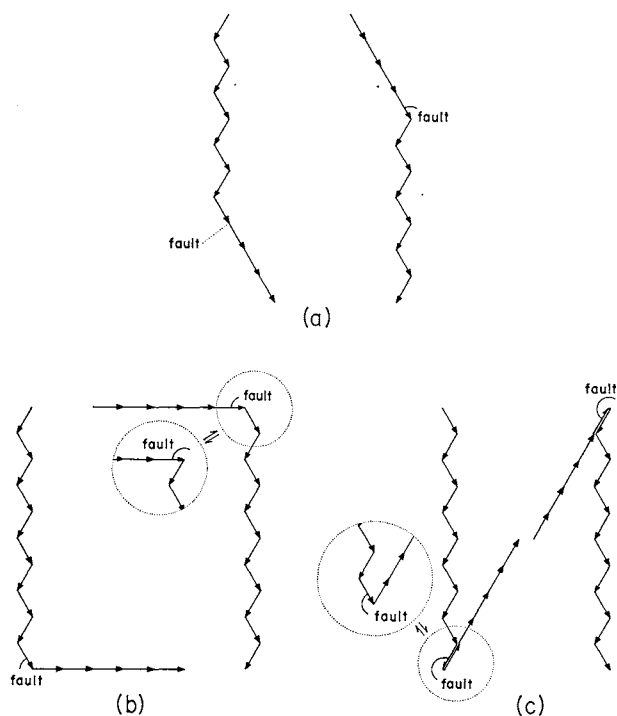


Fig.7. Three epitactic overgrowths of  $2M_2$  and  $1M$  shown by SMITH and YODER's<sup>10</sup> stacking vectors. Alternate interpretations of stacking faults in cases (b) and (c) are shown in circles

$2M_1$  is irreversible<sup>28</sup> and pressure-dependent<sup>29</sup>. The pressure-preference of  $2M_1$  follows from a comparison of single-layer thickness,  $d_{00N}$ ,<sup>30</sup> and volume of  $1M$  subcell,  $V/N$ ,<sup>30</sup> calculated for different muscovites:

	$V/N$	$d_{00N}$
$1M$ <sup>28</sup>	471.537 Å <sup>3</sup>	10.066 Å
$3T$ <sup>24</sup>	467.227	9.990
$2M_1$ <sup>28</sup>	467.096	10.007
$2M_1$ <sup>25</sup>	466.307	9.973

<sup>28</sup> H. S. YODER and H. P. EUGSTER, Synthetic and natural muscovites. *Geochim. Cosmochim. Acta* 8 (1955) 225–280.

<sup>29</sup> B. VELDE, Experimental determination of muscovite polymorph stabilities. *Amer. Mineralogist* 50 (1965) 436–449.

<sup>30</sup>  $N$  is the number of layers in the repeat of a polytype or polymorph.

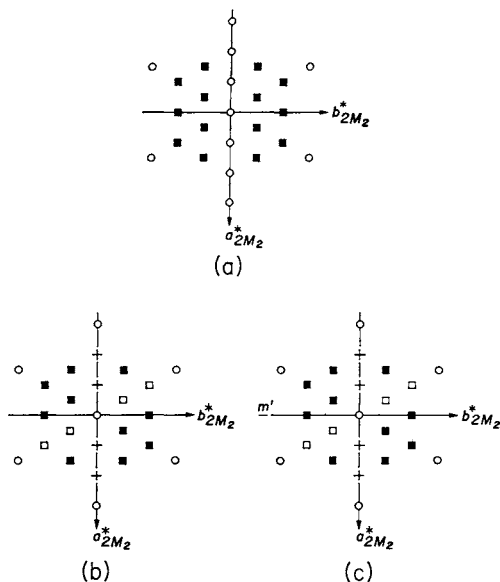


Fig. 8. Reciprocal lattices of  $2M_2$  and  $1M$  in epitactic overgrowths of Fig. 7 projected along  $c^*$ . Symbols as in Figs. 3 and 6. The criteria for (b) and (c) differ only by the presence of symmetry plane  $m'$

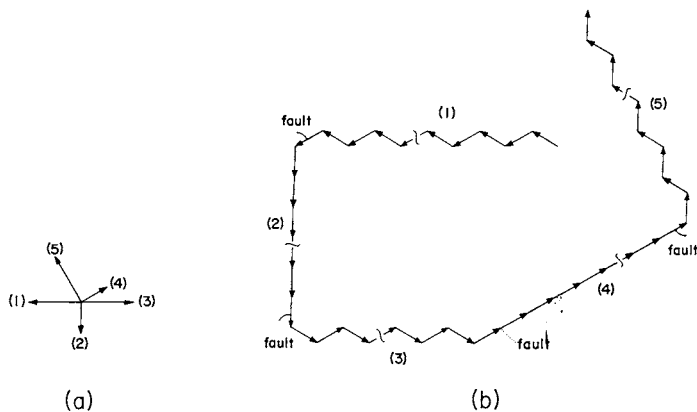


Fig. 9. A complex five-individual overgrowth involving  $2M_2$  and  $1M$  (trilithionite from Radkovice, Czechoslovakia) shown by directions of stacking vectors (a) and as a possible interpretation (b)

All these features indicate polymorphism, which is proven by symmetry differences between single layers in these polymorphs<sup>24,25,31</sup>.

<sup>31</sup> N. GÜVEN, A mechanism of stacking sequences in dioctahedral micas. Carnegie Inst. Wash. Year Book 66 (1968) 492–494.

There are marked differences between muscovite and trioctahedral micas. Trioctahedral micas form stackings with large as well as small repeats; no transformations between such structures are known to date and are unlikely in view of the fact that  $1M$ -subcell volumes within one sample are rigorously, or very close to, identical<sup>2</sup>. There is, however, no evidence that the symmetry of the unit layer is identical in various structures as required in polytypes, but there is also no evidence of the opposite. Accordingly, we use tentatively the term "polytype" when referring to trioctahedral micas.

Trilithionite behaves differently from muscovite and trioctahedral micas. The low number of structures in trilithionite and the very high proportion of  $2M_2$  (not verified in synthetic trilithionite<sup>32</sup>) make one suspect polymorphism. However, the  $d_{00N}$  of  $1M$  and  $2M_2$  tend to be identical<sup>2,33</sup>, as would be among polytypes. The case is more complex still: If  $2M_2$  is a composite of  $A$  and  $B$  layers<sup>34</sup>, it does not have a polymorphic or polytypic relation to  $1M$ . Structure differences between  $A$  and  $B$  lower the symmetry of composite  $A$  and  $B$  structures so that  $2M_2 \rightarrow 2Tc$ ,  $2O \rightarrow 2M$ ,  $6H \rightarrow 6T$  ( $2M$ ,  $2Tc$  and  $6T$  may be polymorphs or polytypes among themselves). Hence I use the word "structure" when referring to trilithionite.

## 2. Polytypes observed in lithium-iron micas

Among the 104 crystals examined, the following polytypes were found (their numbers shown in parentheses):  $1M$  (62),  $2M_1$  (10),  $2M_2$  (10),  $3T$  (7),  $9Tc$  (1),  $5M$  (1),  $12M$  (1),  $14M$  (1). In eleven cases the identity period is larger than eighteen layers, and the repeat could not be resolved with the technique employed. Four of these showed asymmetry in the intensity distribution and are probably triclinic. One of the unresolved polytypes appears to be  $1M_{7-n}$  (120)<sup>26</sup>. Many of the  $1M$ ,  $2M_1$  and  $3T$  polytypes give patterns with weak diffuse streaks parallel  $c^*$ , indicating some randomness in stacking.

Polytypes  $5M$ ,  $9Tc$ ,  $12M$  and  $14M$  have not been reported yet.  $5M$  and  $14M$  are members of the  $[(222)_n 2\bar{2}]$  polytype series<sup>26</sup> with  $n$  equal to 1 and 3, respectively, as was ascertained by comparison

<sup>32</sup> J. L. MUNOZ, Physical properties of synthetic lepidolites. Amer. Mineralogist **53** (1968) 1490–1512.

<sup>33</sup> M. FRANZINI and F. SARTORI, Crystal data on  $1M$  and  $2M_2$  lepidolites. Contrib. Min. Petr. **23** (1969) 257–270.

<sup>34</sup> M. FRANZINI, The  $A$  and  $B$  mica layers and the crystal structure of sheet silicates. Contrib. Min. Petr. **21** (1969) 203–224.

of intensities of diffractions in  $02l$ ,  $04l$ ,  $11l$  and  $22l$  rows with calculated periodic intensity distribution function  $\bar{S}^N$ <sup>27,30,35</sup>. Members of this series  $8M_8$  ( $n = 2$ ), and  $11M$  ( $n = 3$ ) have been known<sup>26</sup>.  $9Tc$  appears to be a member of the  $[(0)_n2\bar{2}]$  series with  $n = 7$ ; intensities of its diffractions were compared to  $\bar{S}^N$  for  $8Tc_1$ <sup>35</sup> and  $14Tc_1$ <sup>26</sup>, as  $\bar{S}^N$  for  $9Tc$  was not available. Other members of this series,  $3Tc_1$  ( $n = 1$ ),  $8Tc_1$  ( $n = 6$ ),  $14Tc_1$  ( $n = 12$ ), and  $23Tc_1$  ( $n = 21$ ) have been known<sup>26</sup>. No stacking sequence for  $12M$  is proposed. Characteristic intensity distribution of the four new polytypes are shown in Fig. 10; cell data, in Table 3.

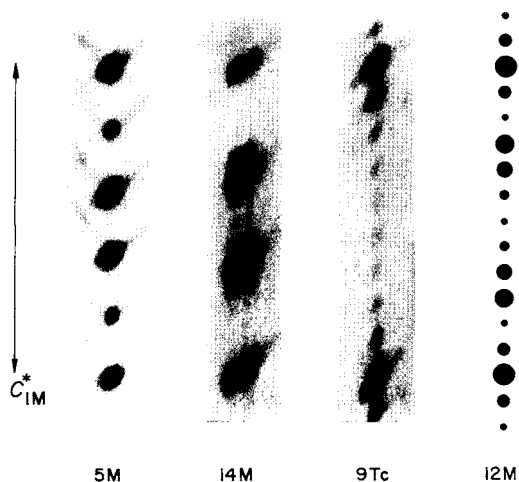


Fig. 10. Intensity distribution in the  $02l$  rows of the four new mica polytypes

With the possible exception of  $12M$  and of the unresolved polytypes, rotations in the stacking sequence of all polytypes observed are  $0^\circ$ ,  $120^\circ$ ,  $240^\circ$  or their combinations. A  $60^\circ$  rotation is present only in  $2M_2$  trillithionite.

Presence of the so-called dioctahedral reflections, i.e.  $0kl$  and  $hhl$  with  $h+k = 6n$  and  $l \neq nN$ <sup>30</sup> and  $h0l$  and  $h3hl$  with  $l \neq nN$ <sup>30</sup>, was verified in all polytypes with more than two layers. They were not found in two-layer polytypes, where  $h0l$  with  $l \neq nN$  would change the diffraction symbol  $C^*/c$  to  $C^*/*$ . Intensities of these diffractions are low, and long exposures are needed to bring them out. Their

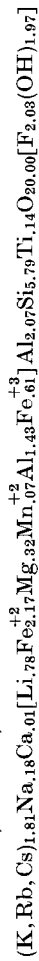
<sup>35</sup> Made available by Dr. M. Ross.

Table 3. Cell data for four new polytypes found in lithium-iron micas

Polytype	Stacking symbol	Space group	a	b	c	$\alpha$	$\beta$	$\gamma$	Sample*
5M	[(222) <sub>1</sub> 22]	C2	5.316 Å ±.005	9.201 Å ±.010	50.000 Å ±.030	—	95° 15' ± 00'	—	23
14M	[(222) <sub>4</sub> 22]	C2	5.281 ±.003	9.158 ±.006	139.35 ±.08	—	95° 09' ± 02'	—	5
9Tc	[(0) <sub>7</sub> 22]	C1	5.384 ±.006	9.299 ±.007	90.61 ±.05	91° 08' ± 02'	94° 49' ± 02'	90° 00' ± 00'	44
12M	?	C*/*	5.303 ±.006	9.174 ±.010	119.65 ±.12	—	94° 52½' ± 02½'	—	29

\* Sample numbers refer to those used in 1,2. Their localities and formulas are as follows:

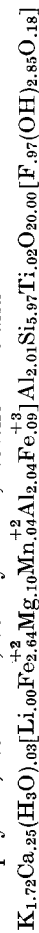
23 — zinnwaldite, Činovec, Czechoslovakia



5 — zinnwaldite, Krupka, Czechoslovakia



44 — siderophyllite, Newcastle, County Down, Northern Ireland



29 — zinnwaldite, Ehrenfriedersdorf, Germany



The cell data were obtained using a precession camera calibrated with quartz and sodium chloride. Each photograph was corrected for film shrinkage or expansion. The  $\pm$  is an estimate of the standard error of the mean. Copper and molybdenum radiations were used, their wavelengths were taken as 1.5418 Å and .7107 Å, respectively.

identification in unresolved polytypes is not possible as they may coincide with diffuse scattering due to a possible  $n \cdot 60^\circ$  rotational disorder<sup>26</sup>.

### 3. Angle beta and polytypism

The behavior of angles in mica cells has received limited attention. Angle beta in monoclinic polytypes is given either in the more correct  $\sim 95^\circ$  ( $\beta'$ ) or less correct  $\sim 100^\circ$  ( $\beta$ ) settings, which are related as  $\tan(\beta' - 90^\circ) = a/2d_{00N} - \tan(\beta - 90^\circ)$ . Beta angle for the  $2M_2$  structure can be chosen only as  $\sim 99^\circ$ . It had been observed<sup>15</sup> that

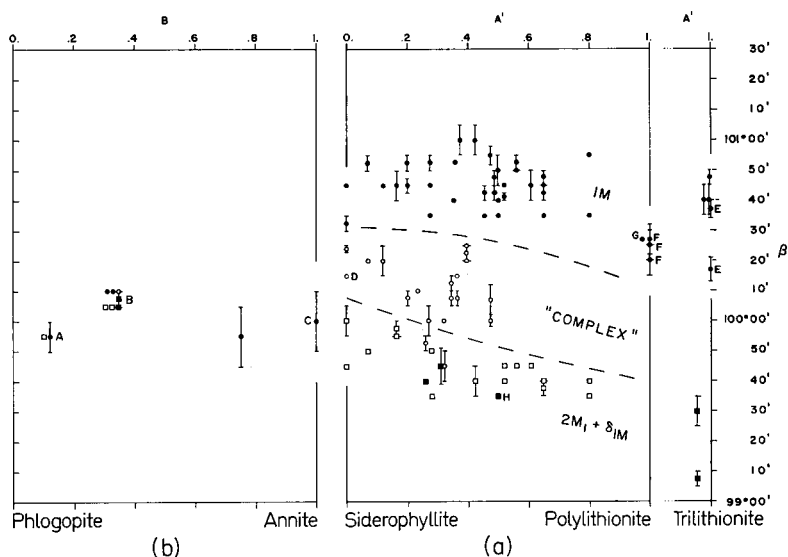


Fig. 11.  $\beta$  angle of  $1M$  subcell of lithium-iron-magnesium micas in the  $\sim 100^\circ$  setting. As composition axes are used  $A' \doteq \text{Li}/(\text{Li} + \text{Fe}^{+2})$  and  $B \doteq \text{Fe}^{+2}/(\text{Fe}^{+2} + \text{Mg})$ , defined in <sup>1</sup>. In (a), areas of  $1M$  (solid circles), "complex" (open circles) and  $2M_1$  (solid squares) and  $\delta$  (open squares) are tentatively separated by broken lines. "Complex" refers to all polytypes other than  $1M$  and  $2M_1$ . A— $1M$  phlogopite from Baikal Lake, U.S.S.R.; B— $1M$ ,  $2M_1$ ,  $4M$  natural and hydrogenated oxy-biotite from Ruiz Peak, New Mexico; C—synthetic  $1M$  ferriannite<sup>6</sup>; D— $3Tc$  siderophyllite<sup>26</sup>; E—synthetic  $1M$  trilithionite<sup>36</sup>; F—synthetic  $1M$  polyolithionite<sup>36</sup>; G— $1M$  "grey lepidolite", Kangerdluarsuk, Greenland, data by TAKEDA in <sup>37</sup>; H—synthetic fluoro-zinnwaldite. Data for E and F are refined powder data, all others are single-crystal data

<sup>36</sup> Dr. J. L. MUNOZ, Written communication.

<sup>37</sup> J. L. MUNOZ, Synthesis and stability of lepidolites. Ph. D. Thesis, Johns Hopkins University, Baltimore (1966).

the beta angle of some micas is close to  $100^{\circ}00'$  and to the "ideal  $\beta$ " =  $\arccos(a/3c)$ . In  $1M$  muscovite<sup>10</sup>, however, the difference between measured beta and "ideal  $\beta$ " is almost  $2^{\circ}$ , in  $2M_1$  muscovite, about  $30'$ . Discussing this in connection with ideality and non-ideality of mica structures, SMITH and YODER<sup>10</sup> implied that muscovite deviates from the ideal structure more than phlogopite whose  $\beta_{\text{meas}} = \arccos(a/3c)$ .

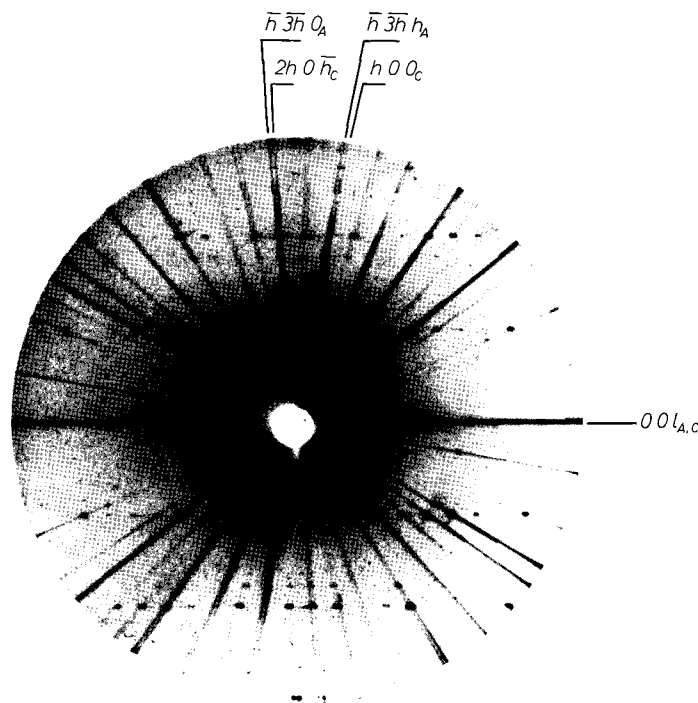


Fig. 12.  $h0l_{1M}$  and  $h3hl_{1M}$  nets as they superpose in an  $h3hl$  net of a  $CA$  twin. The two orientations ( $C, A$ ) give the most intense diffractions on photographs of an unresolved overgrowth in a synthetic fluoro-zinnwaldite. Note weak additional diffractions. Unfiltered molybdenum  $K$  radiation

In the course of the present study, I observed cases similar to the ones cited, and offer the following explanation: In the micas studied, angle  $\beta$  of  $1M$  is either identical with, or larger than, the angle between  $L_{131}^*$  and  $L_{001}^*$  of  $1M$  (denoted  $\delta$ ). Angle  $\beta$  is measured in  $h0l_{1M}$  net,  $\delta$  in  $h3hl_{1M}$  net. In polytypes based on  $n(120^{\circ})$  rotations, angle  $\beta$  is related to  $\beta_{1M}$  and  $\delta$ . The upper extreme is  $1M$ , whose  $\beta = \beta_{1M}$ , the lower extreme is  $2M_1$ , whose  $\beta = \delta$ . The latter

becomes clear if we realize that in photographing the  $h0l_{2M_1}$  net, the x-ray beam follows in fact the  $[3\bar{1}0]$  and  $[\bar{3}10]$  axes of the two layers in  $2M_1$  structure; thus  $h0l_{2M_1}$  and  $h\ 3h\ l_{1M}$  are geometrically identical. Betas of all  $n$  ( $120^\circ$ ) polytypes must then lie between  $\beta_{1M}$  and  $\delta$ . This pattern holds well for lithium-iron micas, the difference  $\beta_{1M} - \delta$  being about  $1^\circ 10'$  (Figs. 11, 12 and 2). This difference is perhaps a measure of non-ideality of their structure. Similar is the behavior of muscovite. In magnesium-iron micas,  $\beta_{1M} \approx \delta$ , and betas for all their polytypes are identical within the error of measurement (Fig. 11).

If the stacking sequence of a polytype is known, the measured angle in its, say,  $h0l$  net can be checked against its estimate. The latter is an average of angles in reciprocal nets that belong to  $1M$  layers participating in the repeat and that face the  $[010]$  direction of the polytype cell. So,  $\beta$  of  $5M$  was estimated as  $95^\circ 19'$ , the measured value being  $95^\circ 15'$  (Table 3). The angle between  $\mathbf{L}_{132}^*$  and  $\mathbf{L}_{001}^*$  of a  $2M_1$  zinnwaldite was estimated as  $100^\circ 15'$ , measured as  $100^\circ 20'$ . Analogously,  $\beta$  of the  $1M$  subcell of  $3T$  and  $1M_r - n(120)$  can be predicted as  $(\beta + 2\delta)/3$ , this being rigorously identical to  $\arccos(a/3c)$ . The "ideality" of this angle does not prove "ideality" of the structure; it is a mere consequence of stacking, irrespective of how "non-ideal" are  $\beta$  and  $\delta$  of  $1M$  layers involved.

If angles predicted differ from those measured, they indicate a structure distortion due to stacking, as is probably the case in muscovite:  $\beta_{1M}$  was found<sup>28</sup> to be  $101^\circ 35' \pm 5'$ ;  $\delta$  was calculated from the data in<sup>28</sup> as  $98^\circ 53'$ ;  $\beta_{2M_1}$  was given in<sup>28</sup> as  $99^\circ 34' \pm 5'$ , in<sup>38</sup> as  $99^\circ 17'$ . It is clear that  $\beta_{2M_1}$  is closer to  $\delta$  than it is to  $\beta_{1M}$ , but it is also clear that the difference between  $\beta_{2M_1}$  and  $\delta$  is too big to be insignificant. It probably is another consequence of polymorphism in muscovite.

Two significant conclusions follow from variation of the beta angle: (i)  $d_{00N}$  is superior to  $c/N$  in cell-parameter plots. (ii) The angular differences represent an additional criterion for identification of twins and epitactic overgrowths (Fig. 12, section V).

## V. Identification of twins and epitactic overgrowths

Twins of the  $1M$  micas can be identified by presence criteria listed in Fig. 3. All cases can be identified if we are able to distinguish

<sup>38</sup> W. W. JACKSON and J. WEST, The crystal structure of muscovite— $\text{KAl}_2(\text{AlSi}_3)\text{O}_{10}(\text{OH})_2$ . Z. Kristallogr. **76** (1930) 211–227.

$m'$  from  $m''$  and  $m$ ; this concerns cases  $e, f$  and  $i, k, l$ . Symbol  $m'$  applies to a geometrically rigorous symmetry plane<sup>39</sup> that can be photographed only in zero-level photographs; it is not a symmetry plane of the twin. Symbol  $m''$  applies to nets formed as an overlap of  $h0l_{1M}$  and  $h3hl_{1M}$  nets; if  $\beta_{1M} \neq \delta$ ,  $m''$  is not a symmetry plane, if  $\beta_{1M} = \delta$ ,  $m''$  cannot be distinguished from  $m'$ . In order to decide between  $m'$  and  $m''$ , accurate angular measurements are essential. Naturally, this criterion fails in micas whose  $\beta_{1M} = \delta$ .

Difficulties associated with differentiation of  $3T$  from a  $CAB$  twin have been known<sup>10,5</sup>. Let us summarize cases permitting a reliable distinction of both. Twinning, and not  $3T$ , is the case (i) if intensities of diffractions in rows parallel to  $c^*$  are uneven, indicating unequal volumes of participating individuals; (ii) if diffractions in rows parallel to  $c^*$  lie on zigzags, indicating an imperfect alignment of  $c^*$  of participating individuals; (iii) if photographs of the " $h0l_{3T}$ " nets show splitting of diffractions like the one in Fig. 12, proving thus the presence of more crystals (note: photographs of an epitactic overgrowth of  $1M$  and  $3T$  may exhibit a similar feature); (iv) if the distances between diffractions in rows parallel to  $c^*$  (in " $hhl_{3T}$ " nets) are not even and approach the case shown in Fig. 13*b*. Inversely, a reliable proof of the presence of  $3T$  is the appearance of "dioctahedral reflections" in the  $h0l_{3T}$  net (used in this study). Naturally, the last resort for differentiation between the two alternatives is a comparison of measured and calculated intensities<sup>4</sup>.

Identification of epitactic overgrowths involving two individuals ( $1M$ ,  $2M^{21}$ ) can be based on presence criteria of Figs. 6 and 8. Examination of  $h0l_{2M}$  and  $0kl_{2M}$  reveals all information needed. It should be borne in mind that patterns of case  $b$  in Figs. 5, 6 do not differ from those of  $2M_1$  by presence of additional diffractions. Epitactic overgrowths can be distinguished from  $2M_1$  if the  $h0l_{2M_1}$  exhibits splitting like that of Fig. 12; epitaxy is to be suspected if the  $hhl$  and  $0kl$  nets of  $2M_1$  show evidence of a strong  $1M$  subcell.

If the twin and epitaxy criteria fail to account for all diffractions on the photographs, the case should be solved from as many reciprocal nets as possible. Criteria for twins of more layer structures or for overgrowths more complex than given in Figs. 4–8 were not explored systematically; I consider their derivation impractical and premature at this stage. Complex overgrowths should be represented by

<sup>39</sup> Symmetry planes in photographs of twins relate the geometrical positions of diffraction spots, not necessarily their intensities.

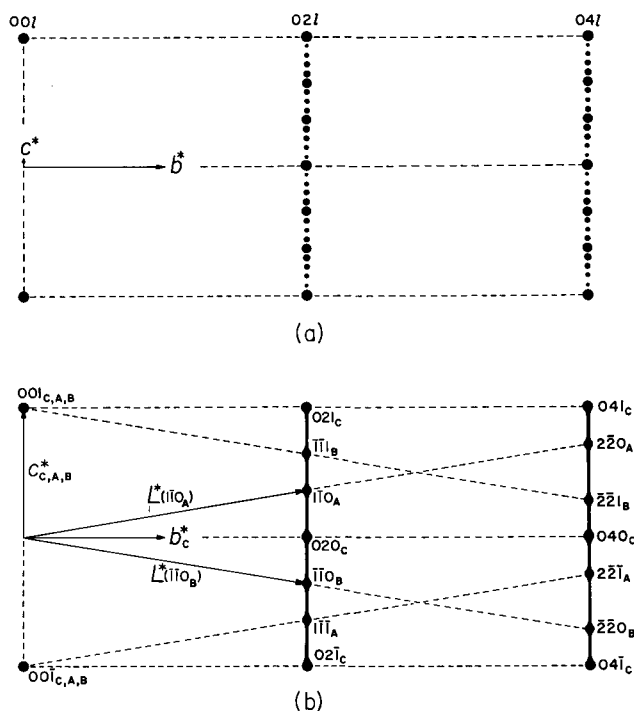


Fig. 13. An idealized drawing of a part of the  $0kl$  net of  $14M$  polytype (a) and of a similar net of a twin (b). The twinning is combined with diffuse scattering in directions parallel  $c^*$ . Case (a) is drawn according to photographs of  $14M$ , (b) according to photographs of a  $C\bar{B}A\bar{C}B\bar{A}$ ,  $C\bar{B}A\bar{C}B$  or  $C\bar{B}AB$  twin in sample 38 (Table 2). To make the drawing simpler, only diffractions from orientations  $C$ ,  $A$ ,  $B$  are labeled

vectors rather than as an interpretation, unless there is a reason for doing so.

Only one hint for identification of polytypes with a  $3T$  subcell from twins was observed; it is illustrated in Fig. 13. Twinning combined with diffuse scattering, which is fairly common in lithium-iron micas, may be mistaken for a complex polytype, such as  $14M$ . There is similarity between  $02l_{14M}$  and the corresponding row of the twin, but the cases give away their true nature in  $04l_{14M}$  and the corresponding twin row.

## VI. Geological application

All polytypes observed in lithium-iron micas on the siderophyllite-polyolithionite join are based on rotations of  $n(120^\circ)$  as had been reported<sup>16</sup>. No other relation between polytypism and composition of

these micas has been observed. Little or no dependence of polytypism on parameters like temperature and pressure can be expected, as follows from coexistence of several polytypes in one specimen and from the existence of epitaxial overgrowths between two polytypes.

There appears to be a relation between polytypism of these micas and the mode of their occurrence. Rotational disorder (in randomly stacked polytypes) is believed to be a product of random edge dislocations<sup>40</sup>, which are more likely to occur in conditions of fast and chaotic growth. Regular complex stacking that is related to screw dislocations<sup>40</sup> indicates a slower growth rate. This is the pattern observed: Randomly stacked and unresolved polytypes were found in large crystals from pegmatitic occurrences; resolved complex polytypes, in small crystals from hydrothermal veins and greisens. Most rock-forming micas crystallize as  $1M$  or other simple polytypes. Polytypism thus appears to be a function of growth conditions. Growth conditions are, I believe, responsible also for epitaxy between different mica polytypes.

If the high-temperature preference for twins were proven, it would indicate that twinning is governed by another factor than polytypism and epitaxy. More data are needed to clarify the relation between polytypism, twinning, and epitaxy in lithium-iron micas.

The behavior of trilithionite is different from that of other lithium-iron micas: the  $2M_2$  structure is based on a  $60^\circ$  rotation, and these micas show no sign of random or complex stacking even though they come from typical pegmatites. The data available do not permit any interpretation of these phenomena.

### Acknowledgments

I am indebted to Dr. M. ROSS and Dr. H. P. EUGSTER for many stimulating discussions and suggestions. Unpublished data were made available by Dr. M. ROSS and Dr. J. L. MUNOZ. Valuable discussions on some aspects of the problem were held with Dr. G. DONNAY, Dr. J. D. H. DONNAY and Dr. M. FRANZINI. Dr. H. P. EUGSTER and Dr. G. W. FISHER read drafts of the manuscript.

As a part of a Ph. D. Thesis project, the research was aided by NSF Grant GP-5064, H. P. EUGSTER principal investigator; by stipends and fellowships from the Johns Hopkins University; and by the Ústřední ústav geologický. All support is gratefully acknowledged.

<sup>40</sup> A. J. VERMA and P. KRISHNA, *Polymorphism and polytypism in crystals*. J. Wiley & Sons, Inc., New York, London, Sydney (1966).